Wen et al., http://www.jcb.org/cgi/content/full/jcb.201105109/DC1

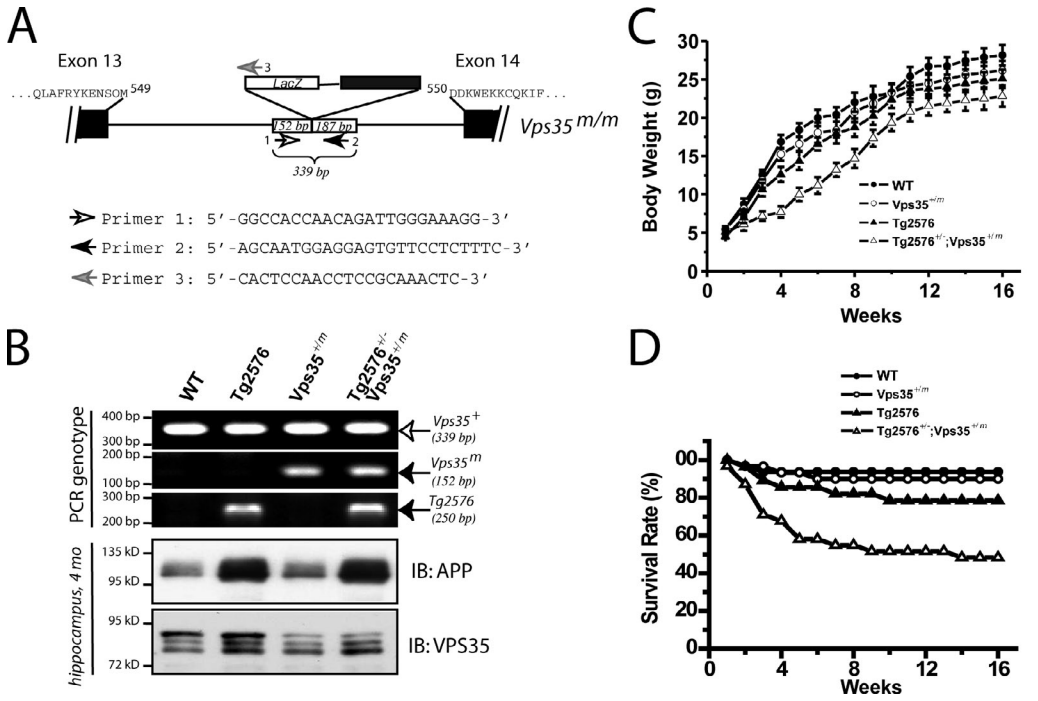

Figure S1. **Generation of Tg2576$^{+/-}$;Vps35$^{+/m}$ mutant mice.** (A) Diagram of the retrotranspon insertion in Vps35 gene. Exons 13 and 14, the surrounding intron, and the location of genotyping primers are shown diagrammatically. Primer sequences are also indicated. (B) Genotyping and expression of AP-Pswe and VPS35 expression in the indicated mutant hippocampus. IB, immunoblotted. (C) Reduced body weight in 1–8-wk-old Tg2576$^{+/-}$;Vps35$^{+/m}$ mutant mice. Data as mean ± SEM (n = 12–17) are shown. (D) Decreased life span in Tg2576$^{+/-}$;Vps35$^{+/m}$ mutant mice.

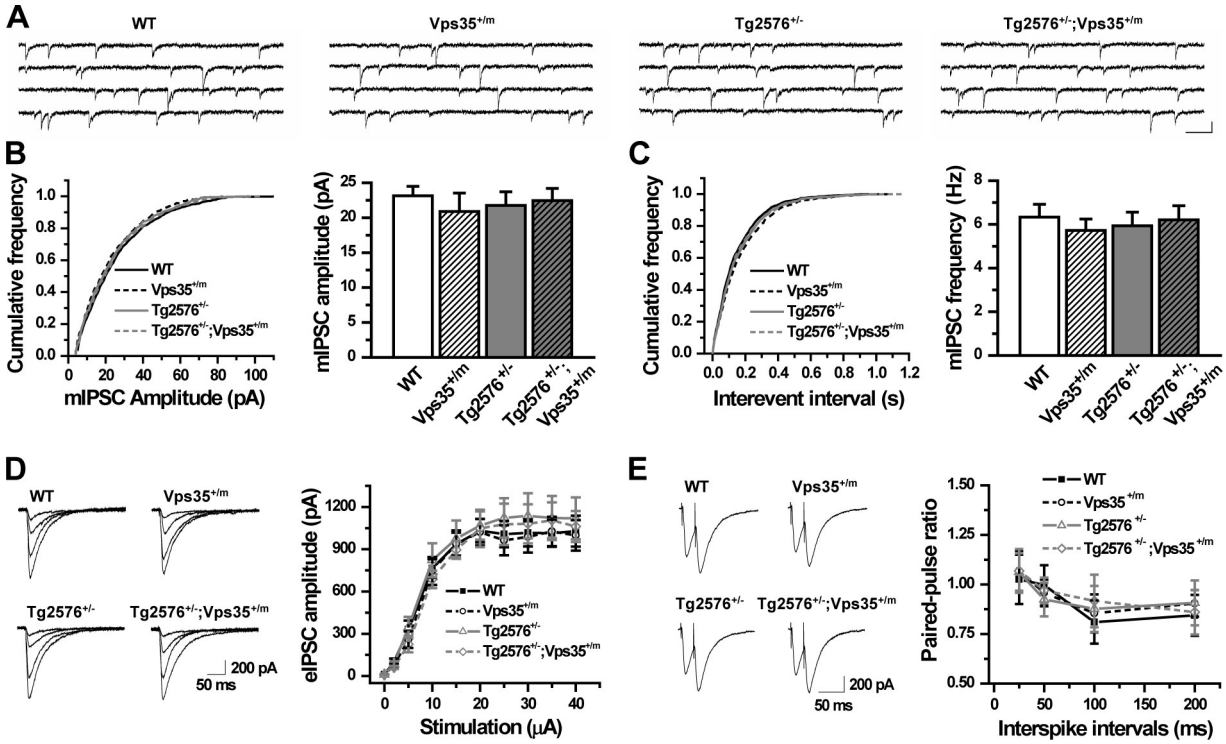

Figure S2. **Normal inhibitory synaptic transmission in hippocampal CA1 pyramidal neurons of Tg2576$^{+/-}$;Vps35$^{+/m}$ mice.** (A) Representative traces of mIPSCs. Bar, 100 ms, 40 pA. (B) Cumulative distribution plots (left) and mean amplitude (right) of mIPSCs. (C) Cumulative frequency plots of the interevent interval (left) and quantitative analysis of the frequency (right) of mIPSCs. (D) Representative traces of eIPSCs (2, 5, and 10 µA and saturating stimulus intensities; left) and quantification analysis of the IPSC amplitude to stimulus intensity (right). (E) Paired-pulse ratio analysis. Representative traces (left) and quantification analysis (right). Data were obtained from the whole-cell recordings of the hippocampal CA1 pyramidal neurons from the four groups of mice (2 mo old) including Tg2576$^{+/-}$, Vps35$^{+/m}$, and Tg2576$^{+/-}$;Vps35$^{+/m}$ mice and WT controls. (B–E) Data were analyzed by one-way ANOVA followed by Dunnett's test (for mean mIPSC amplitude and frequency and for paired-pulse ratio), Kolmogorov–Smirnov test (for mIPSC cumulative histograms), and repeated measures ANOVA (for eIPSC amplitude). Mean ± SEM is shown. $P > 0.05$. n = 11–13.

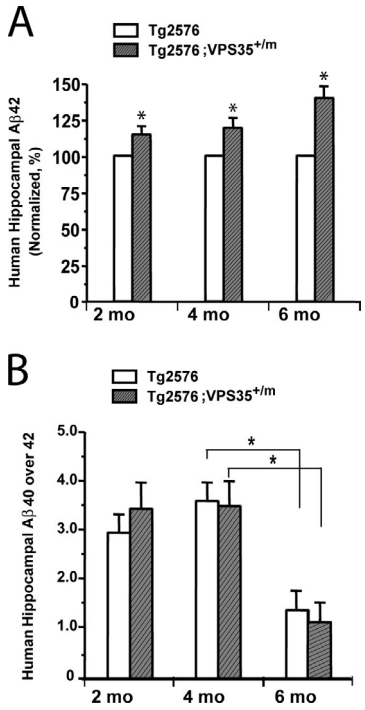

Figure S3. **Increase of $A\beta_{42}$ in young adult $Tg2576^{+/-}$;$Vps35^{+/m}$ hippocampus without a change of the ratio of $A\beta_{40}$ versus $A\beta_{42}$ in the mutant mice.** (A) Increase of human $A\beta_{42}$ in 2–6-mo-old $Tg2576^{+/-}$;$Vps35^{+/m}$ hippocampus (compared with $Tg2576^{+/-}$; data were normalized against $Tg2576^{+/-}$ and presented as a percentage). (B) No change of the ratio of human $A\beta_{40}$ over $A\beta_{42}$ between $Tg2576^{+/-}$ versus $Tg2576^{+/-}$;$Vps35^{+/m}$. However, a significant decrease was observed in 6-mo-old mice as compared with that of 2–4-mo-old mice. (A and B) Data, shown as mean ± SEM, were analyzed by one-way ANOVA followed by Dunnett's test. *, $P < 0.01$. $n = 4$ for each of the genotypes.

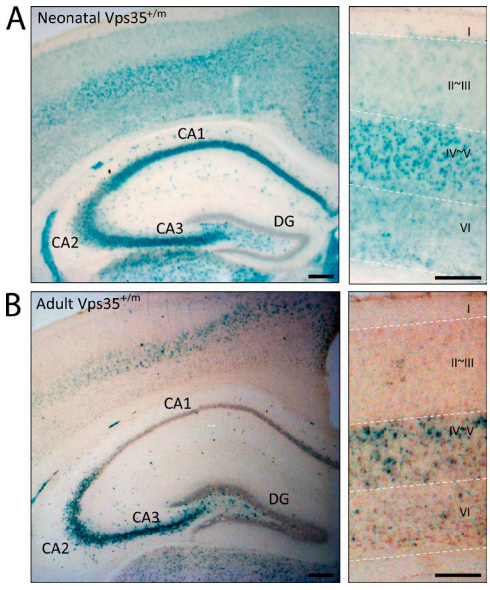

Figure S4. **Age-dependent reduction of Vps35 expression in CA1 and cortical neurons.** (A and B) Detection of enzymatic LacZ activity in neonatal (A) and adult (B) $Vps35^{+/m}$ hippocampus and cortex. At the neonatal brain, LacZ activity was detected in CA1–3 hippocampus and layers II–VI but was enriched in layer IV–V cortical neurons (A). However, at adult age (>3 mo old), LacZ activity became restricted in the CA2–3 hippocampus and layer IV–V cortical neurons (B). Layers I–VI in cortex, DG, and CA1–3 in hippocampus are indicated. Bars, 200 µm.

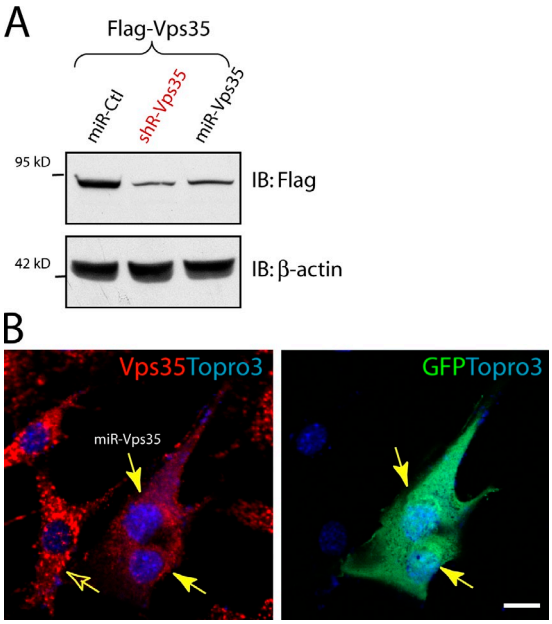

Figure S5. **Suppression of Vps35 expression by both shRNA and miRNA-Vps35.** (A) Western blot analysis showing Vps35 expression in HEK293 cells transfected with the indicated plasmids. IB, immunoblotted. (B) Expression of endogenous Vps35 was suppressed by miRNA-Vps35 (miR-Vps35) in transfected NLT cells. NLT cells were transiently transfected with miRNA-Vps35 plasmid, which encodes GFP as well as miRNA of Vps35. Transfected cells were fixed and immunostained with anti-Vps35 antibody (rabbit polyclonal). GFP indicates the expression of the miRNA-Vps35 plasmid. The open arrow indicates VPS35 distribution in untransfected cells, and closed arrows indicate reduced Vps35 expression in miRNA-Vps35–transfected cells. Bars, 20 µm.